sustainability

MDPI

Article

CFD Investigation of Vehicle's Ventilation Systems and Analysis of ACH in Typical Airplanes, Cars, and Buses

Behrouz Pirouz [1,*], Domenico Mazzeo [1], Stefania Anna Palermo [2], Seyed Navid Naghib [1], Michele Turco [2] and Patrizia Piro [2]

[1] Department of Mechanical, Energy and Management Engineering, University of Calabria, 87036 Rende, CS, Italy; domenico.mazzeo@unical.it (D.M.); navid.naghib@gmail.com (S.N.N.)
[2] Department of Civil Engineering, University of Calabria, 87036 Rende, CS, Italy; stefania.palermo@unical.it (S.A.P.); michele.turco@unical.it (M.T.); patrizia.piro@unical.it (P.P.)
* Correspondence: behrouz.pirouz@unical.it; Tel.: +39-0984-496542

Abstract: The simulation of the ventilation and the heating, ventilation, and air conditioning (HVAC) systems of vehicles could be used in the energy demand management of vehicles besides improving the air quality inside their cabins. Moreover, traveling by public transport during a pandemic is a concerning factor, and analysis of the vehicle's cabin environments could demonstrate how to decrease the risk and create a safer journey for passengers. Therefore, this article presents airflow analysis, air changes per hour (ACH), and respiration aerosols' trajectory inside three vehicles, including a typical car, bus, and airplane. In this regard, three vehicles' cabin environment boundary conditions and the HVAC systems of the selected vehicles were determined, and three-dimensional numerical simulations were performed using computational fluid dynamic (CFD) modeling. The analysis of the airflow patterns and aerosol trajectories in the selected vehicles demonstrate the critical impact of inflow, outflow, and passenger's locations in the cabins. The CFD model results exhibited that the lowest risk could be in the airplane and the highest in the bus because of the location of airflows and outflows. The discrete CFD model analysis determined the ACH for a typical car of about 4.3, a typical bus of about 7.5, and in a typical airplane of about 8.5, which were all less than the standard protocol of infection prevention, 12 ACH. According to the results, opening windows in the cars could decrease the aerosol loads and improve the low ACH by the HVAC systems. However, for the buses, a new design for the outflow location or an increase in the number of outflows appeared necessary. In the case of airplanes, the airflow paths were suitable, and by increasing the airflow speed, the required ACH might be achieved. Finally, in the closed (recirculating) systems, the role of filters in decreasing the risk appeared critical.

Keywords: HVAC; CFD; car; bus; airplane; airflow; ACH; IAQ; COVID-19

check for updates

Citation: Pirouz, B.; Mazzeo, D.; Palermo, S.A.; Naghib, S.N.; Turco, M.; Piro, P. CFD Investigation of Vehicle's Ventilation Systems and Analysis of ACH in Typical Airplanes, Cars, and Buses. *Sustainability* **2021**, *13*, 6799. https://doi.org/10.3390/su13126799

Academic Editors: Alessandro Franco and Tomonobu Senjyu

Received: 21 April 2021
Accepted: 10 June 2021
Published: 16 June 2021

Publisher's Note: MDPI stays neutral with regard to jurisdictional claims in published maps and institutional affiliations.

Copyright: © 2021 by the authors. Licensee MDPI, Basel, Switzerland. This article is an open access article distributed under the terms and conditions of the Creative Commons Attribution (CC BY) license (https://creativecommons.org/licenses/by/4.0/).

1. Introduction

Many researchers have analyzed the efficiency of air conditioners (AC), particularly the vehicle producers, to reduce energy consumption and greenhouse gas emissions [1]. Marshall et al. analyzed the thermal management strategies for the vehicle, and their results determined the high impact of HVAC and ventilation on the energy demands, especially in electric vehicles [2]. Suárez et al. analyzed the ventilation and the HVAC system in a railway vehicle with a CFD simulation. They modeled different scenarios in summer and winter, and the results established the methodology for this type of analysis [3].

The experimental analysis of Kale et al. showed the complex airflow inside buses with open windows and determined that the speed of airflow could be about 0.1 of the bus speed [4]. Mathai et al. analyzed the microclimate inside the cabin. Their findings revealed that open windows could increase or decrease the transmission pathways based on the location of the infection source and the open windows [5]. In another study, Gajewski analyzed the indoor air quality in a bus with fresh air during its journeys, focusing on the

CO_2 concentration. The study results determined that the concentration of CO_2 is not fixed during a trip. Because of less fresh air at the beginning of the journey, the CO_2 value could be about 2.5 times more than the permitted value [6].

Shehadi et al. investigated the airflow and turbulence characteristics inside aircraft cabins to decrease the risk of contaminated airborne particles and improve the monitoring. They analyzed Boeing 767 aircraft experimentally by using tracer gas and theatrical smoke. The results determined the dominant air circulations inside the cabin. The main air circulation was cross-section circulation, and the second, with a decreasing trend in the longitudinal direction, affected approximately three rows [7].

Another subject that needs to be considered in the analysis of the AC systems in the vehicle is the health risk, particularly during respiratory pandemics like COVID-19. There are several analysis criteria for respiratory pandemics [8–11]. Outbreaks of respiratory diseases, such as influenza, Middle East respiratory syndrome (MERS), severe acute respiratory syndrome (SARS), and COVID-19, have caused huge negative impacts on all activities worldwide [5]. The analysis determined that using HEPA filters and UV light could improve indoor air quality [12–15]. However, previous studies showed that HVAC filters in the vehicles are often heavily contaminated, which subsequently could carry the harmful particles into the cabins. Therefore, installing a high-efficiency filter and air purifier units could decrease the health risk just in the case of periodic replacement [16,17].

Zhu et al. investigated the air quality in the bus system. They measured the indoor CO_2 level and particles, and their results showed the impact of occupancy conditions. In addition, the analysis of the CO_2 level determined that, usually, the bus ventilation system could not be sufficient to decrease the air pollutants produced by passengers, which can increase the risk of airborne transmitted diseases during the journey [18]. In another study, Zhu et al. analyzed the risk of airborne influenza infection in public transport by using a CFD-based numerical simulation. The simulation results showed the same infection risk for both the air-recirculation mode and the non-air-recirculation mode. The analysis showed that the efficiency of the air-recirculation system with a HEPA filter was nearly equal to the non-air-recirculation system with the refresh air mode [19].

The analysis of HVAC systems depends on numerous parameters [20–22]. Moreover, there are many indoor air quality (IAQ) standards and guidelines such as the WHO, the European air quality guidelines [23,24], and the American Society of Heating, Refrigerating and Air-Conditioning Engineers (ASHRAE) standards [25,26]. The IAQ standards and guidelines are mostly about air quality and pollutant emission, determining the threshold values for some parameters [27–29]. However, the transport of odors and fumes, viruses, and bacteria and the transmission of respiratory infections such as H1N1, Ebola, and COVID-19 have been detected on flights and other vehicles, which could result in health hazards for passengers, cabin crews, or drivers [7,30–33]. For monitoring the indoor air quality, such as in cabins, one method could be the use of measurement devices, and, for health purposes particularly due to airborne diseases, a simple method is the use of CO_2 concentration indicators. The indoor CO_2 load also depends on the passengers, and the increase in CO_2 level could show low ACH [34–36].

The previous studies show that further investigations about the airflow patterns and particle trajectories inside the vehicle cabins could be useful in decreasing the health risk. According to the literature review, the simulation of the ventilation and the HVAC systems of the vehicles could show the airflow pattern and the ACH, and the results can be used in the balance for energy demand management of the vehicles besides improving the air quality inside cabins and decreasing the passengers' health risk. Moreover, the results can be applied in improving the monitoring and controlling of systems. Although there are some case study analyses for the HVAC systems of different vehicles separately, there is no study that compared the airflow and the ACH in different vehicle, which shows the novelty of the current study. The average values that were used in this study make the outcomes more reliable as the results were not limited to any specific model of vehicles.

Therefore, this study aimed to analyze the cabin airflow pattern for three vehicles, including an airplanes, buses, and cars, and to investigate ACH by CFD simulation to improve IAQ. Moreover, the second goal of the study was to show the application of CFD simulation in improving design elements of HVAC systems such as the vent location, the AC loads, and the airflow rate, besides the passenger placement. Although the medical analysis and transmission of the virus are beyond the scope of the present study, it could be useful in decreasing the health risk as it predicts the aerosol trajectory in the vehicles.

In this study, the main factors in analysis of the HVAC systems in the three vehicles including cars, buses, and airplanes were first investigated. Second, different case studies were evaluated, and the average values of the dimension, the airflow speed, and the airflow rate (based on 14 case studies) of the vehicles were determined. Third, the geometry and boundary conditions of the models were defined and validated according to the selected case studies. Fourth, the validated models were used for airflow analysis and ACH. Finally, the results were compared to each other and some suggestions to decrease the health risk in the vehicle cabins were provided.

2. Materials and Methods

The CFD solver model is used to analyze the cabin's airflow pattern, ACH, and the trajectory of aerosols for three vehicles, including airplanes, buses, and cars. The analysis flowchart is presented in Figure 1.

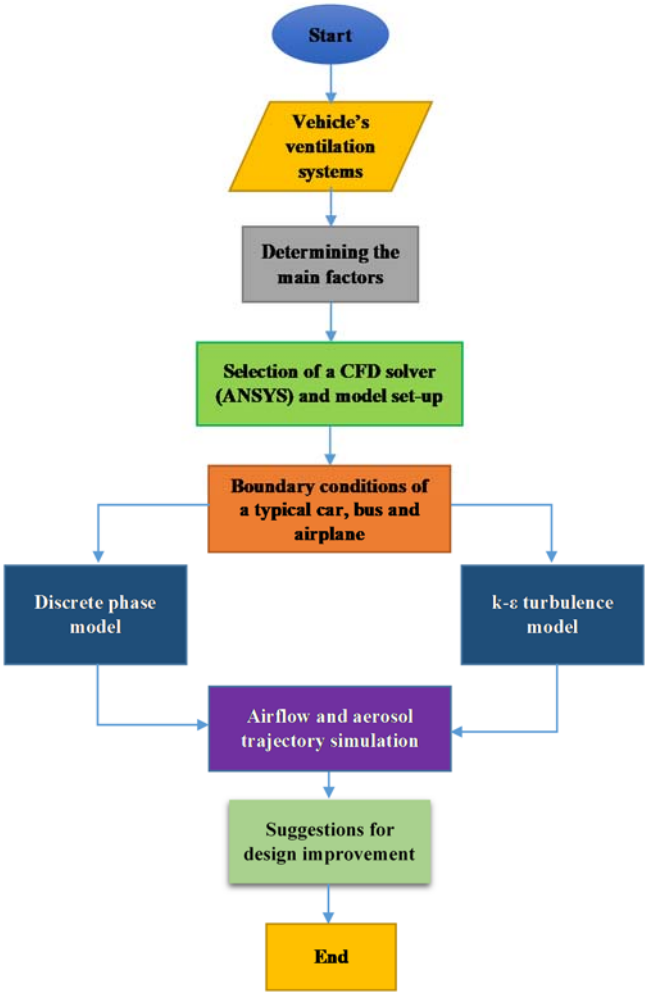


Figure 1. Analysis flowchart for cabin airflow simulation in three vehicles.

The correlations among the health risk and the indoor parameters were approved, and the monitoring of the relative humidity (RH), CO_2, and T was suggested for improving the IAQ [37]. The main factors that affect IAQ in the vehicles included the humidity percentage, CO_2, T, the airflow rate and direction, the type of the utilized air filter [38–40], the seat arrangement, and the displacement of ventilation [19,41]. The main approaches for airflow pattern analysis include experimental measurements and CFD simulations [42,43]. In general, to simulate and estimate the parameters, there are several methods, including mathematical, statistical, and numerical techniques [44–49]. Thus, we used the numerical technique in this study.

2.1. Governing Equations

The main equations in the CFD analysis were Equations (1)–(3). Equations of motion can be used to predict the particle or aerosol trajectory in a discrete phase. The trajectory of a particle such as droplets could be predicted through particle force balance Equations (4) and (5).

Continuity:

$$\frac{\partial \rho}{\partial t} + \nabla . (\rho v) = S_m \tag{1}$$

Momentum:

$$\frac{\partial \rho}{\partial t} + \nabla . (\rho v v) = -\nabla p + \nabla . (\tau) + \rho g + F \tag{2}$$

Energy:

$$\frac{\partial}{\partial t}(\rho E) + \nabla . (v(\rho E + p)) = \nabla . \left(k_{eff} \nabla T - \sum_j h_j J_j + \left(\tau_{eff} . v \right) \right) + S_h \tag{3}$$

$$\frac{du_p}{dt} = F_D(u - u_p) + \frac{g_x(\rho_p + \rho)}{\rho_p} + F_x \tag{4}$$

$$F_D(u - u_p) = \frac{18\mu}{\rho_p d_p^2} \frac{C_D Re}{24} \tag{5}$$

where:

ρ: fluid density; p: pressure; T: temperature; u: fluid phase velocity
u_p: particle velocity; ρ_p: particle density; Fx: additional forces; C_D: drag coefficient
μ: molecular viscosity; Re: relative Reynolds number
$F_D(u - u_p)$: drag force per unit particle mass

2.2. Case Studies and Boundary Conditions

The three-dimensional models of cars, buses, and airplanes were developed according to similar case studies and the available information. To define the boundary conditions in our CFD models, we evaluated the boundary conditions in different case studies, and we selected the average values of dimension, airflow, and temperature for a typical car, bus, and airplane. The dimensions and airflow rates and speeds in five cars, four buses, and four airplanes, and the selected boundary conditions are presented in Table 1.

To define the boundary conditions in the second part of the analysis, discrete phase modeling, the average diameter and speed of the of the aerosol particles in a human sneeze was selected. The human respirational aerosol diameter was between 0 to 100 µm, on average 5 µm, and the aerosol speed in respiration was 0.12–1 m/s; and for a cough and a sneeze was between 4.2 to 11.2 m/s, on average 10 m/s with a duration of 0.5 s [50–53]. Therefore, the aerosol diameter of 5 µm with a speed of 10 m/s and duration of 0.5s was used for the boundary condition.

Table 1. Boundary conditions for CFD analysis.

Vehicle.	Case Study	Dimensions (m)			Airflow Rate (m^3/s)	Airflow Speed (m/s)	Refs.
		Length	Width	Height			
Car	Fayazbakhsh and Bahrami (2013)	3	1	1.5	0.01	-	[1]
	Khatoon and Kim (2020)		2.65 m^3		-	0.16	[54]
	Fišer and Pokorný (2014)	-	-	-	0.02–0.05	2.6–5.8	[55]
	Alexandrov et al. (2001)	-	-	-	-	0.5	[56]
	Danca et al. (2018)	2.8	1.5	1.2	-	0.5–1	[57]
	Typical car	2.5	1.2	1.2	0.06	1	[1]
Bus	Yang et al. (2020)	11.6	2.6	2	-	3	[50]
	Bilgili et al. (2017)	13.7	2.6	3.5	0.05–0.5	-	[58]
	Yang et al. (2015)	9	2.4	2.4	-	2–5	[59]
	Gürbüz et al. (2016)	11.8	2.5	3	0.19	-	[60]
	Typical bus	12	2.5	3	0.3	2	[2]
Airplane	Garner t al. (2003)	56.40	5.9	2.5	-	1	[61]
	Müller and Scholz (2007)		200 m^3		-	1–2	[62]
	You et al. (2016)	-	3.5	2.2	33 ACH	1.44	[63]
	Rai and Chen (2012)	-	4.9	2	0.2	2.6	[64]
	Talaat et al. (2021)	28	3.5	4	-	0.5	[33]
	Typical airplane	40	4.4	2.2	0.3	1.5	[3]

[1] Selected dimension for a typical car; [2] a typical bus; [3] a typical airplane.

2.3. CFD Model Set-Up

The model details, including the geometry of the vehicles and locations of inlets/outlets, are shown in Figures 2–8. The models represent the entire cabins of the three vehicles with some passengers inside. We tried to generate the geometry of the vehicles' cabins accurately. The passengers' human bodies were designed with simplified details to decrease the uncertainty and error in the mesh, as suggested in previous studies [33,65].

To decrease the simulation error, we followed the suggested methodology and considerations in the previous case studies. The base mesh and set-up of the discrete model was done according to the recent studies on aerosol transmission [33,66–68]. To solve the Navier–Stokes equations in the simulation model, the k−ε turbulence method was used as the performance has been verified in similar case studies [68–72]. For simulation, we used a detailed 3D-CFD model in the steady condition, and for the CFD analysis, we used the ANSYS Fluent package.

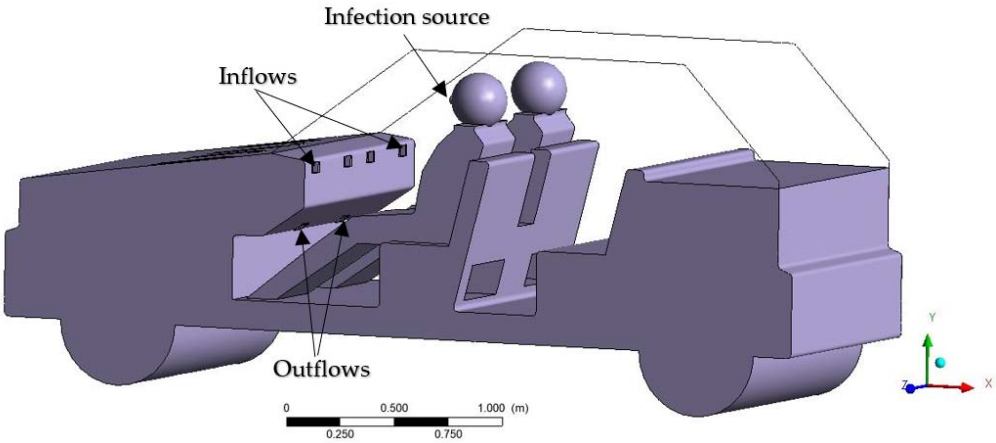


Figure 2. The geometry of the selected typical car.

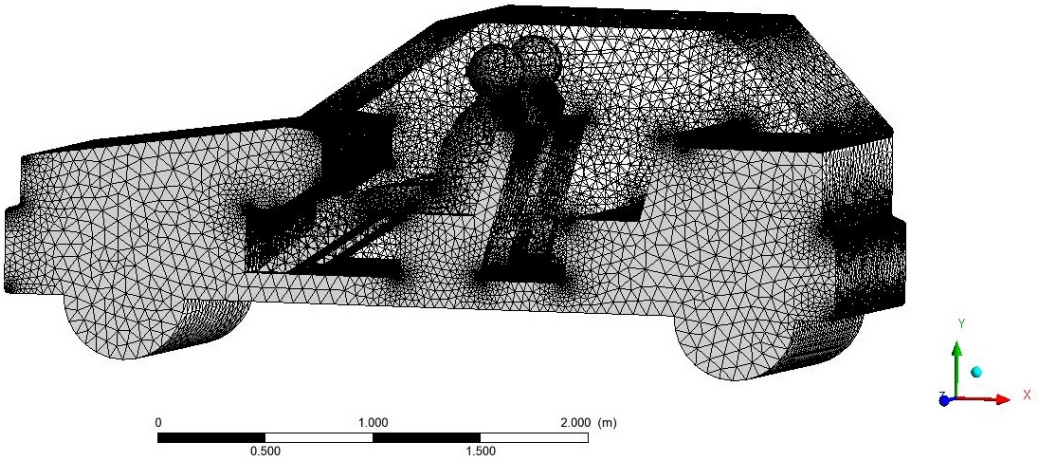


Figure 3. Mesh of the selected typical car.

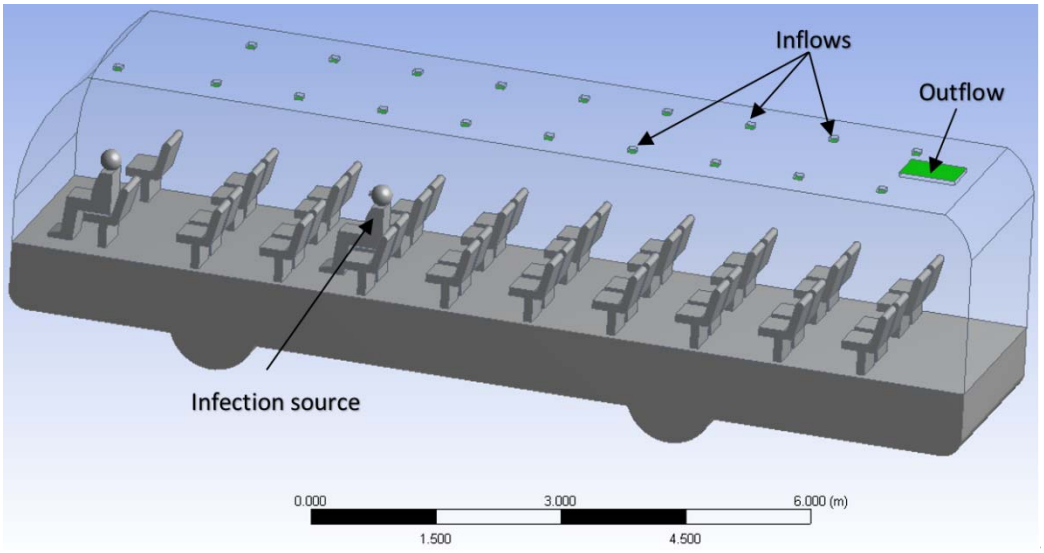


Figure 4. The geometry of the selected typical bus.

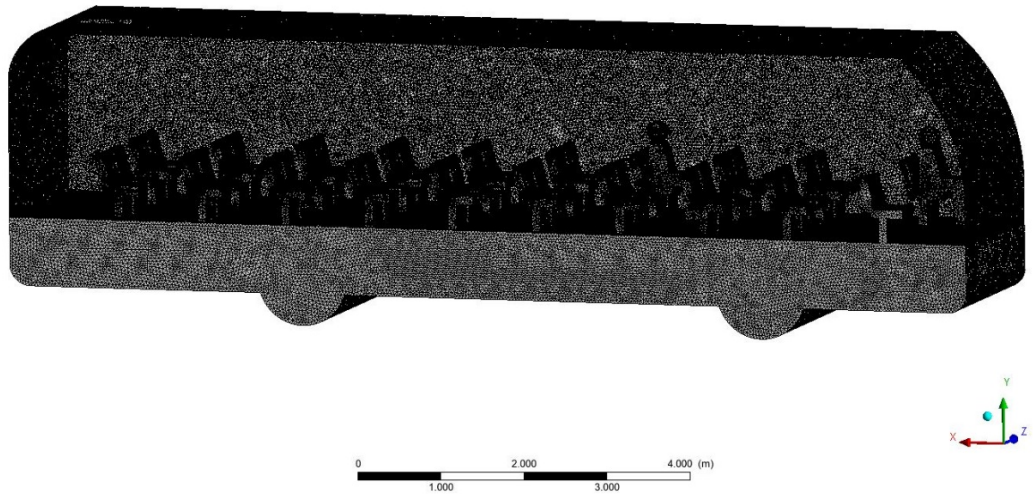


Figure 5. Mesh of the selected typical bus.

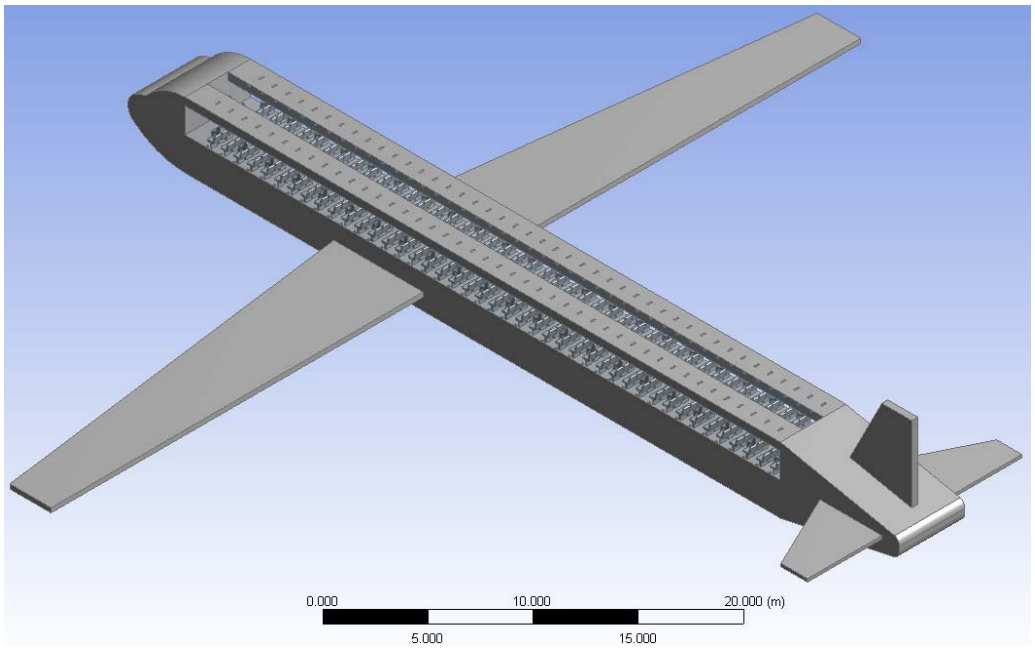


Figure 6. The geometry of the selected typical airplane.

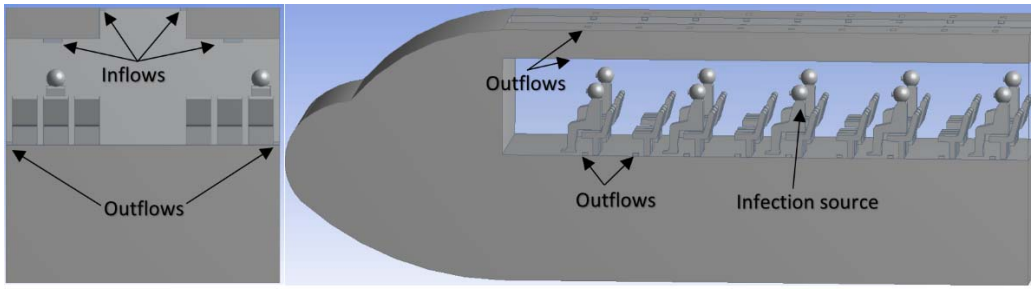


Figure 7. Computational model set-up of the selected typical airplane.

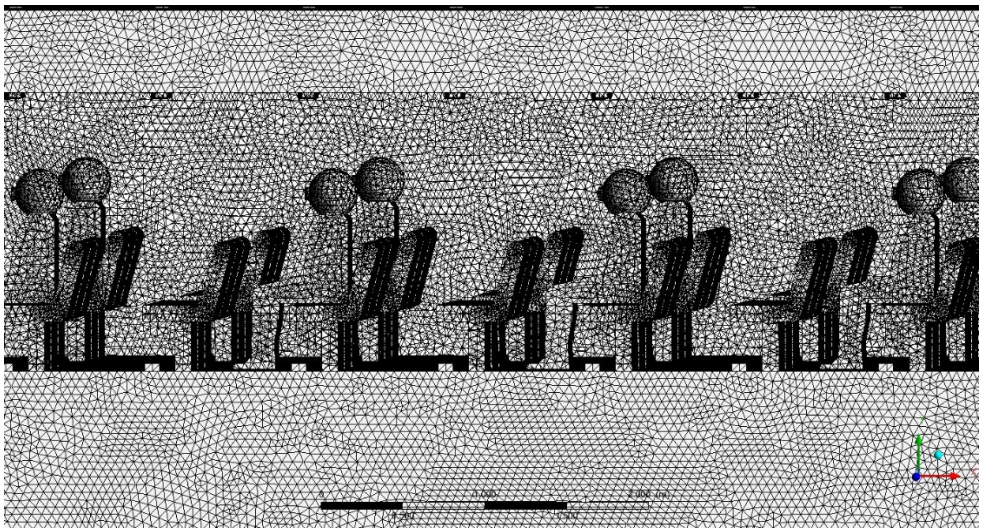
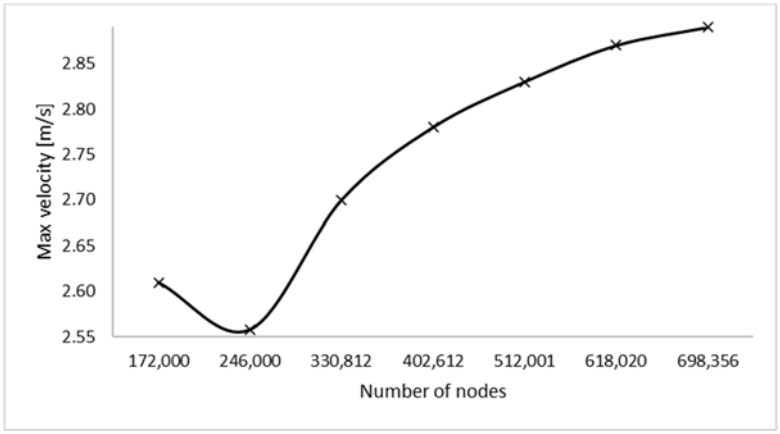
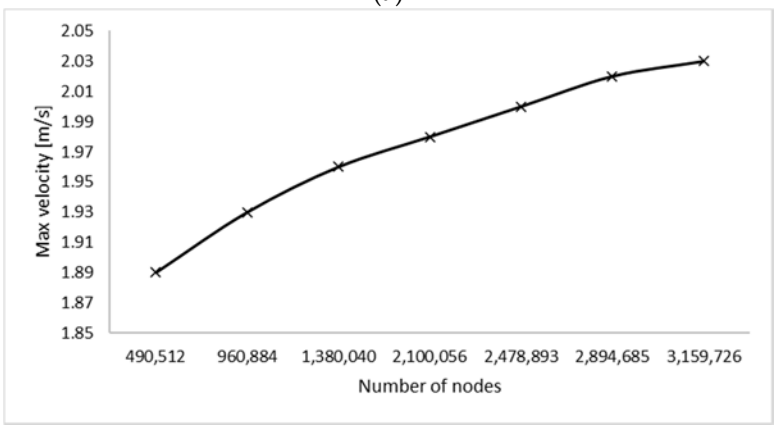


Figure 8. Mesh of the selected typical airplane.

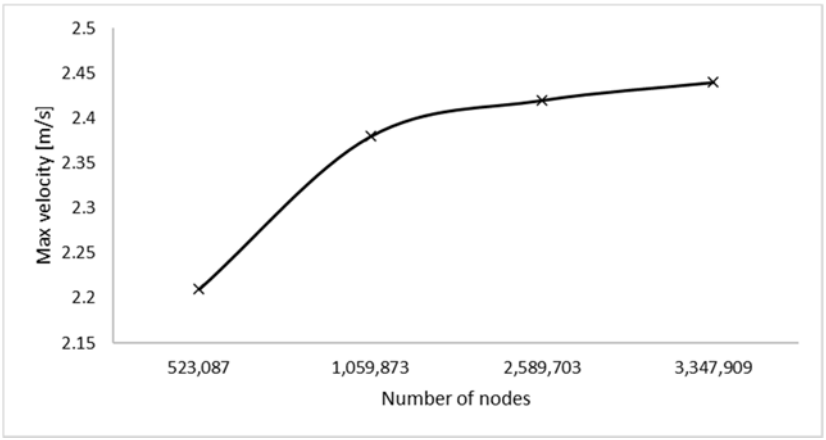
Mesh sensitivity analysis is presented in Figure 9, and details of the final selected mesh is presented in Table 2.



(**a**)



(**b**)



(**c**)

Figure 9. Mesh sensitivity analysis (**a**) car; (**b**) bus; (**c**) airplane.

Table 2. Mesh details in the three selected vehicles.

Case Study	Nodes	Elements (Tetrahedra)	Skewness	Orthogoonal Qiality
Car	512,001	2,704,775	0.241	0.853
Bus	2,478,893	9,725,140	0.221	0.860
Airplane	3,347,909	18,949,720	0.222	0.860

The details of the solution set-up for the three models are presented in Table 3.

Table 3. Model solution set-up details.

Item	Solution Set-Up				
Solver	Type			Pressure based	
	Velocity formulation			Absolute	
	Gravity			−9.81	
Time	Airflow analysis	Steady	Iteration	Car	800
				Bus	1000
				Airplane	1000
	Discrete analysis	Transient	Time step (s)/ Number of time step/max iteration	Car	1/1200/20
				Bus	1/1000/20
				Airplane	1/1000/20
Model	Viscous			k-epsilon	
	Discrete phase				
Material	Air, water liquid				
Boundary condition	Inlet			Velocity	
	Outlet			Pressure outlet	
	Injection			Velocity	
	Surrounded surface			Wall	
Solution	Standard initialization				

For the verification of the numerical analysis, the models were validated initially based on the velocity profile of the measurement data in the previous studies of similar case studies, and then the simulations were completed for the selected boundary conditions. The results of the validation are shown in Figure 10. The used case studies for the validation were as follows:

- The airflow model of the car was validated based on the experimental studies of Khatoon and Kim [54] and Danca et al. [57].
- The bus CFD model was validated based on the studies of Yang et al. [50] and Zhu et al. [19].
- The airplane CFD model was validated based on the experimental analysis by Shehadi et al. [7] and simulation of the Boeing 737 airplane by Talaat et al. [33].

2.4. Main Assumptions and Hypothesis in the CFD Modelling

The main assumptions in this study were as follows:

- The movement of passengers and flight attendants in the bus and airplane were not considered in the analysis;
- It was assumed that passengers were sitting upright with facing front;
- The validation of the models by similar case studies would not affect the main results;
- The average diameter of the respiration aerosol would not affect the main results;
- The models were based on the HVAC system, with full fresh inflow, and the opening windows or recirculation system were not considered in this study.

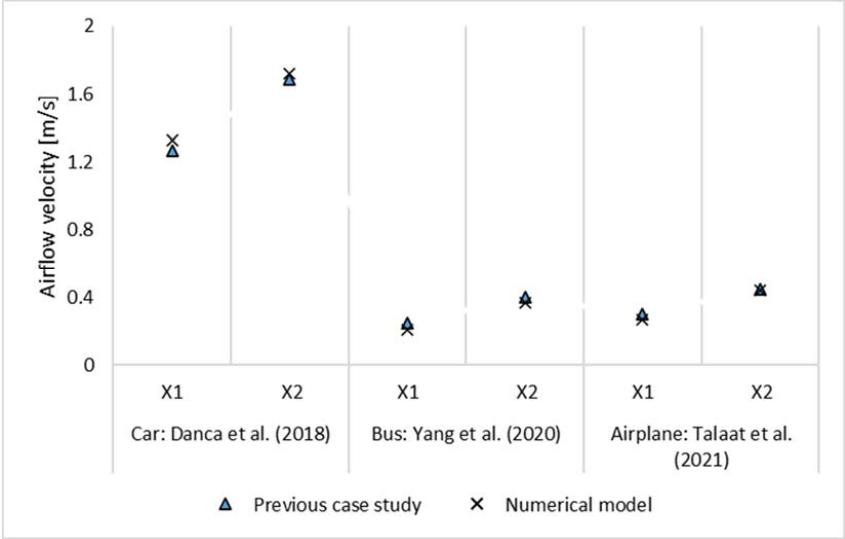


Figure 10. Validation of the models according to the previous case studies.

3. Results and Discussion

3.1. Cabin Airflow Analysis in the Selected Vehicles

In this section, the airflow path, the trajectory of contaminated aerosols, and the ACH in the selected vehicles were simulated. The simulations were based on the use of an HVAC system and were completed according to the defined boundary conditions. The cabin airflow patterns in the selected vehicles are shown in Figures 11–17.

The analysis of the selected vehicles showed the critical impact of inflows' and outflows' locations on the airflow's patterns. Moreover, the results revealed the importance of passenger locations in the cabins. Therefore, it seems that the lowest infection risk based on the airflow paths could be in the airplane, and the highest risk in the bus could be due to the locations of inflows/outflows and the number of passengers.

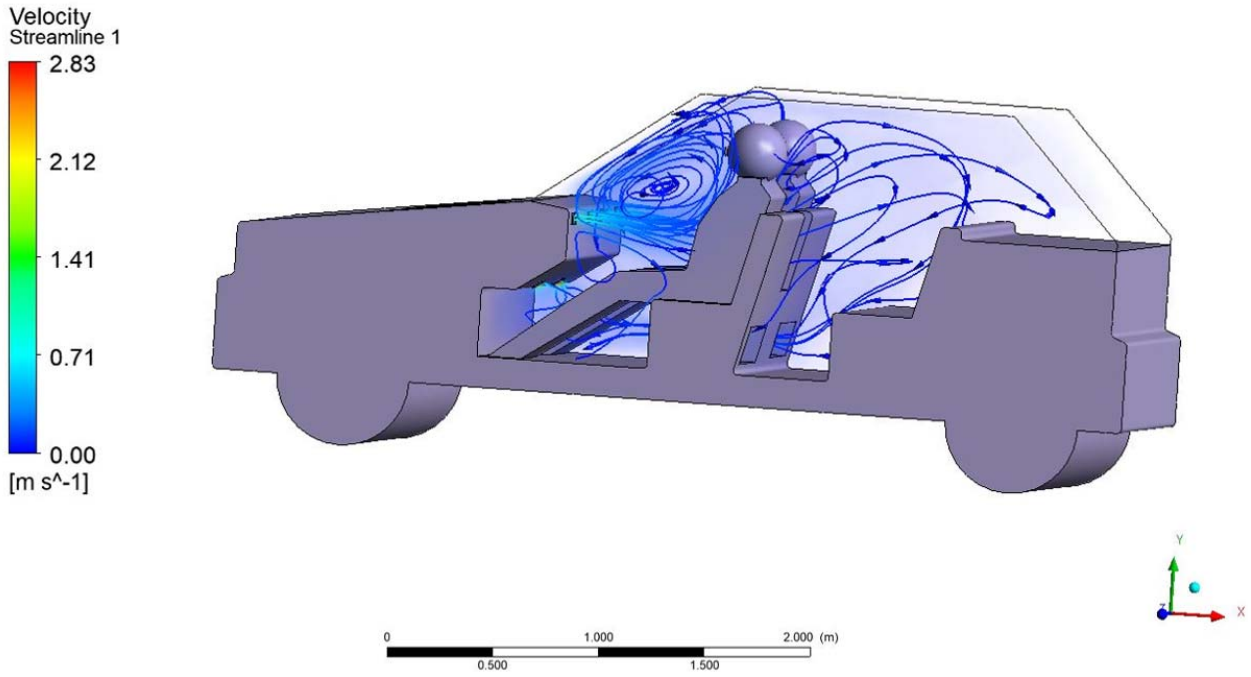


Figure 11. Airflow streamlines in the selected typical car.

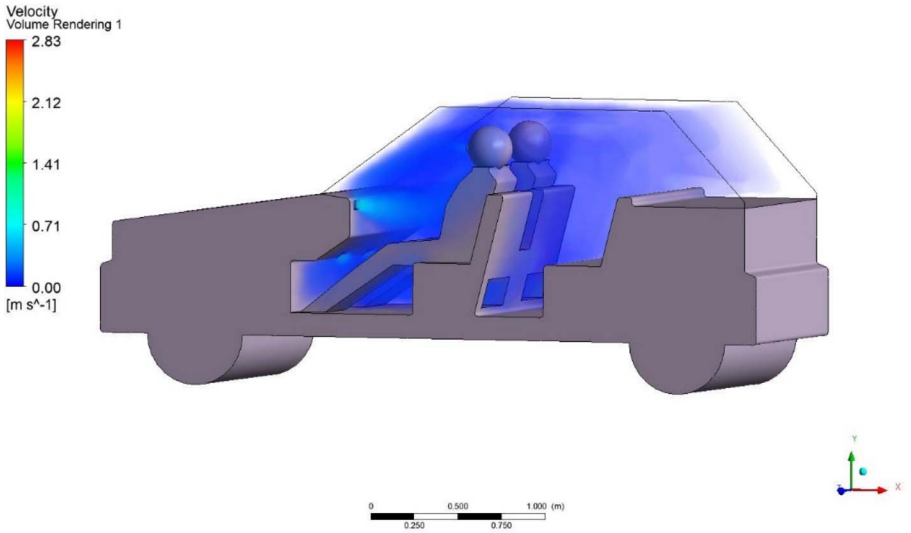


Figure 12. Airflow velocity in the selected typical car.

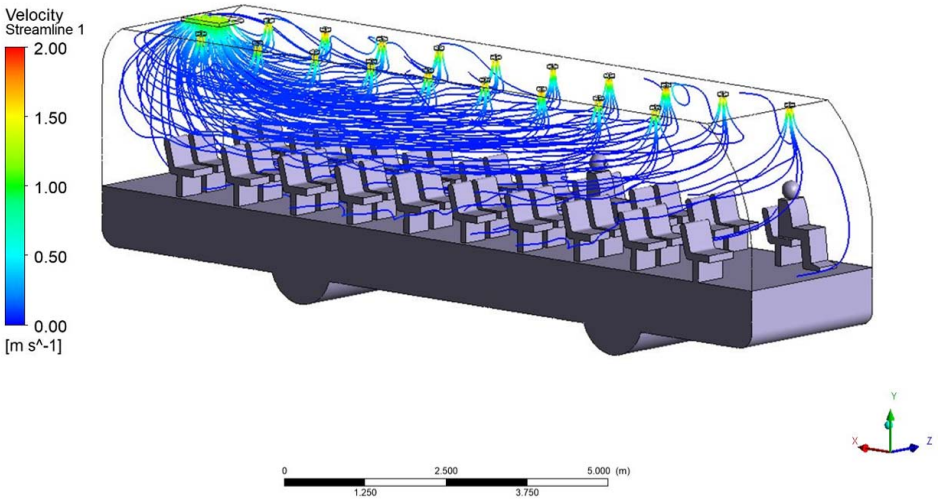


Figure 13. Airflow streamlines in the selected typical bus.

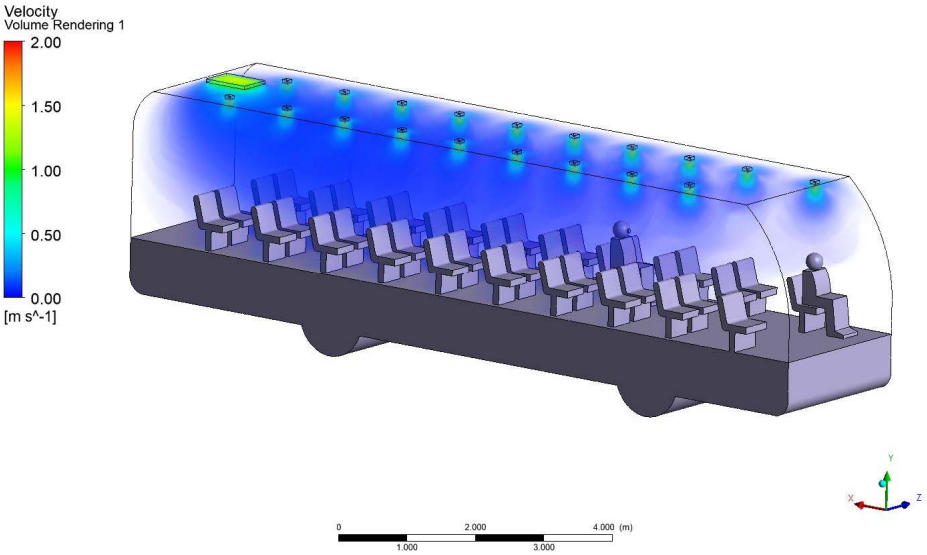
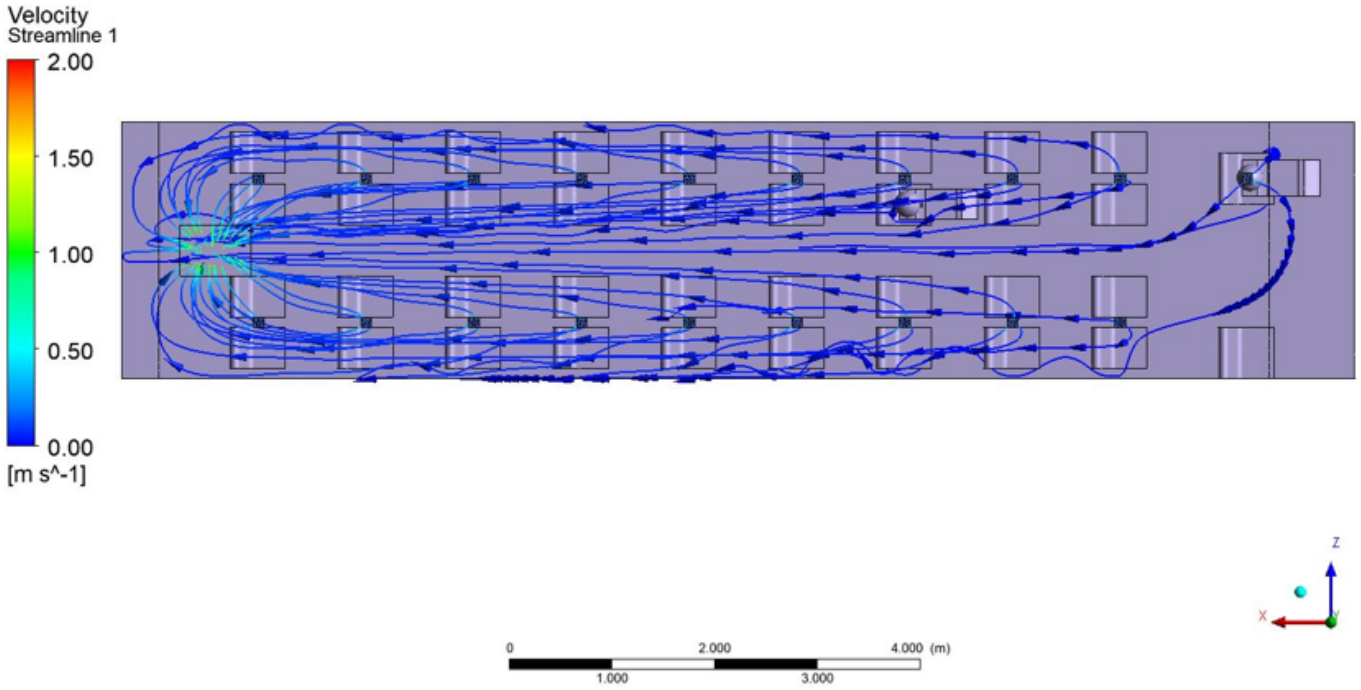
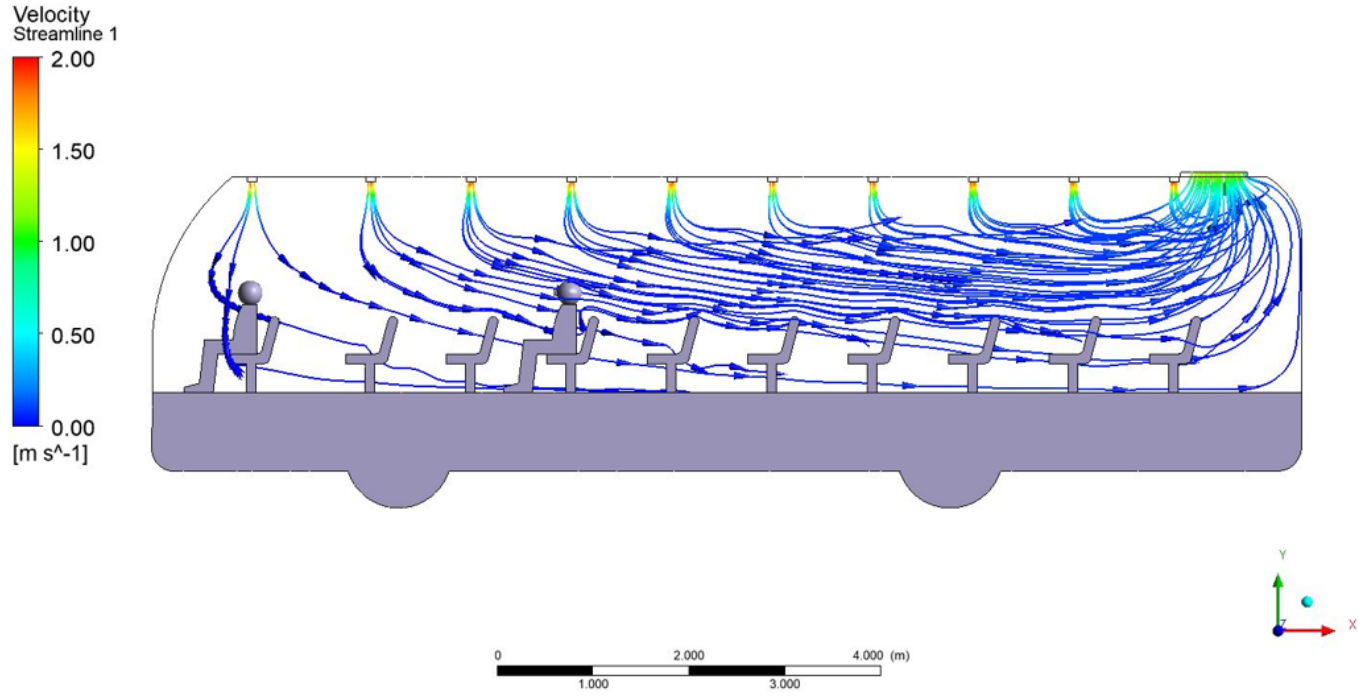


Figure 14. Airflow velocity in the selected typical bus.



(**a**)



(**b**)

Figure 15. Airflow in the selected typical bus (**a**) top view; (**b**) side view.

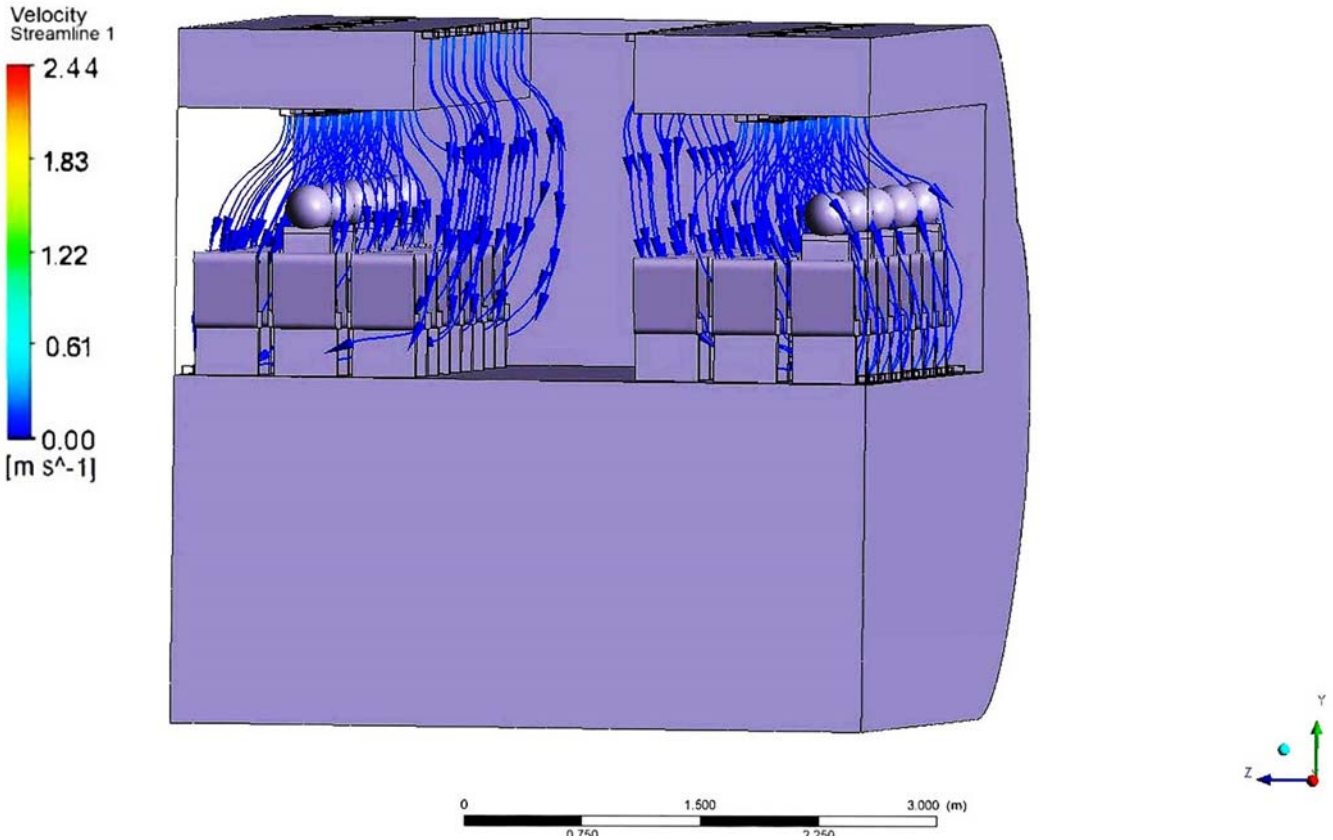
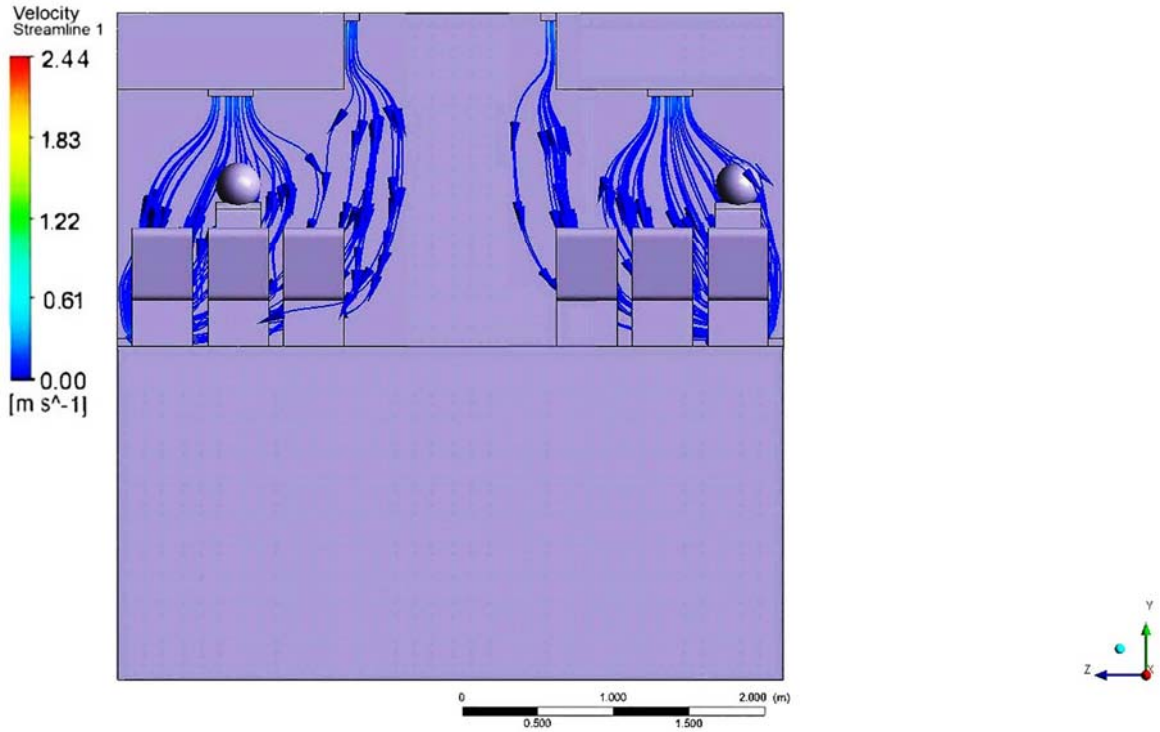
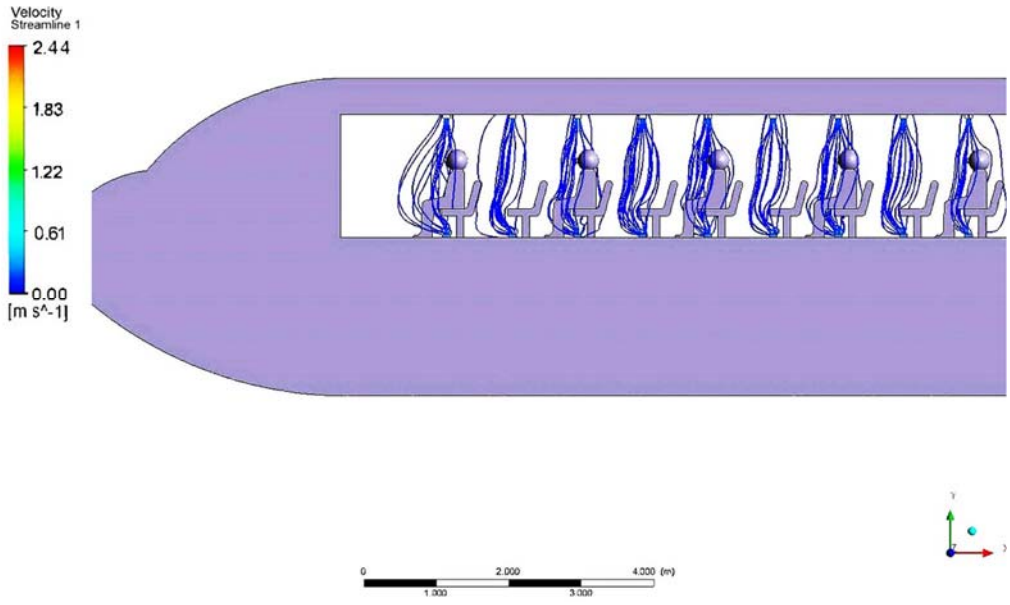


Figure 16. Airflow streamlines pattern in the selected typical airplane.



(**a**)

Figure 17. *Cont*.



(**b**)

Figure 17. Airflow in the selected typical airplane (**a**) side view; (**b**) airflows in the different rows.

3.2. Trajectory of Contaminated Aerosols and ACH Inside Vehicle Cabins

In this section, to check the ACH in the three vehicles, the discrete model analysis was applied. The trajectory of contaminated aerosols in the vehicles are shown in Figures 18–20, and the discrete phase modeling results are presented in Figures 21–23. The aerosol movement was based on the size and airflow speed, and the results of "Particle Traces" are reported in the figures and videos (Supplementary Materials).

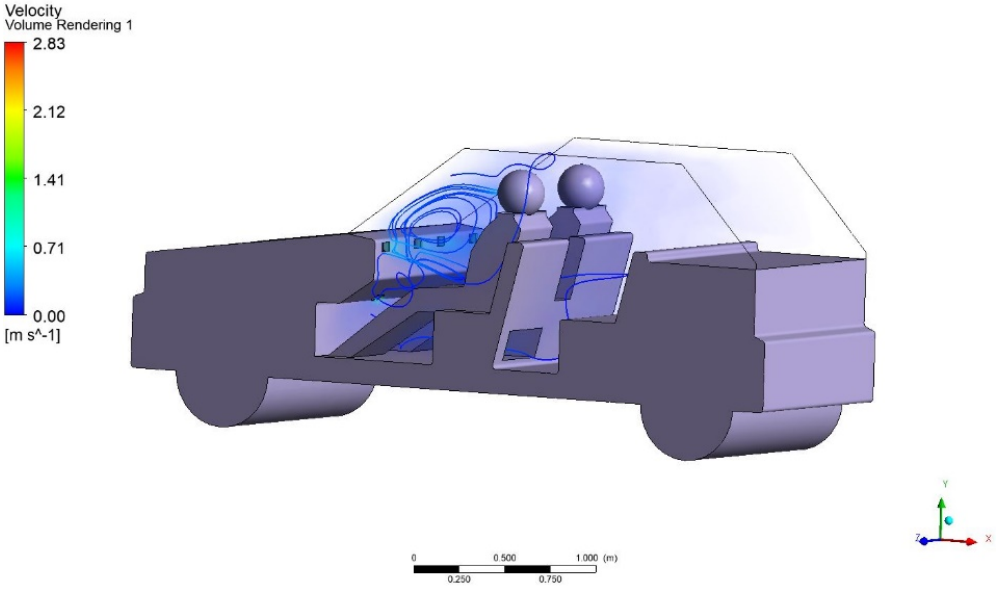


Figure 18. The trajectory of respiration aerosols in the selected typical car.

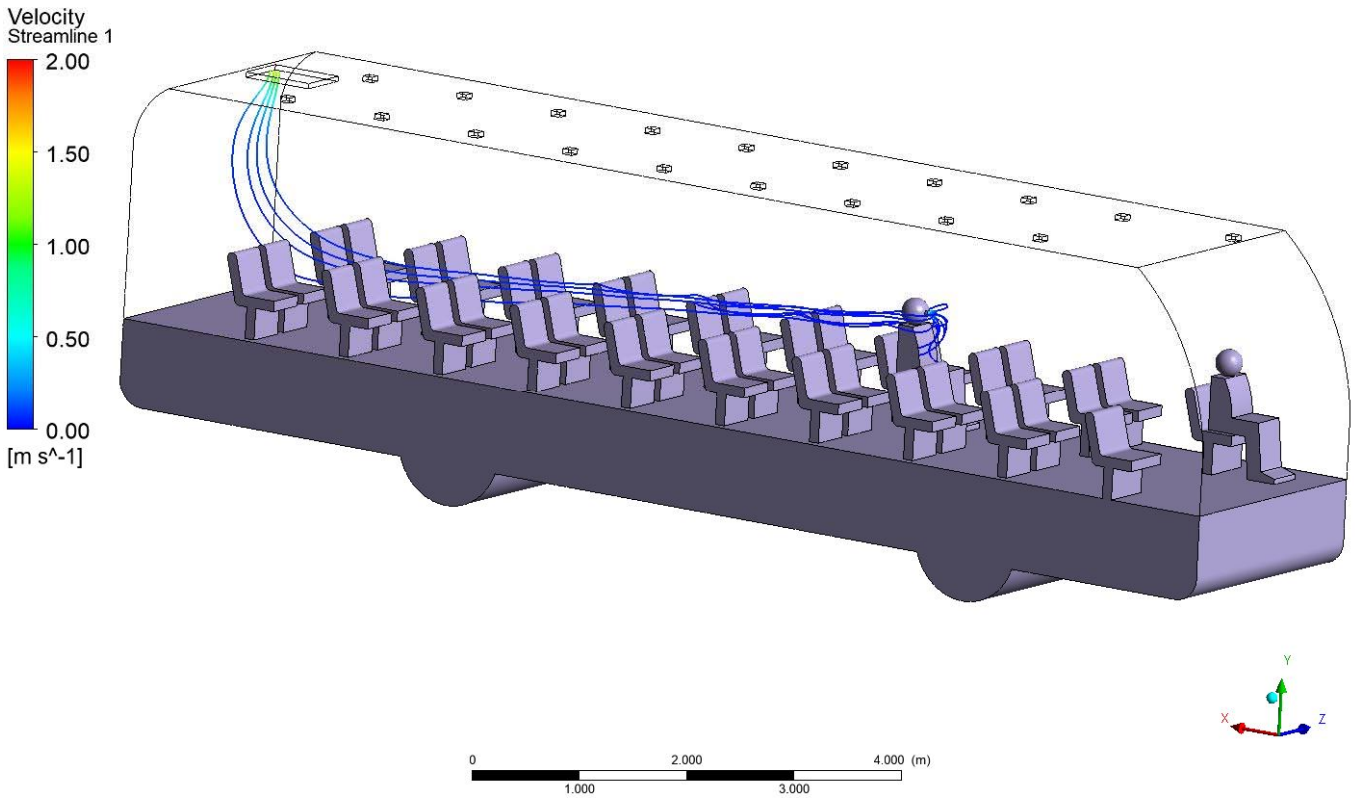


Figure 19. The trajectory of respiration aerosols in the selected typical bus.

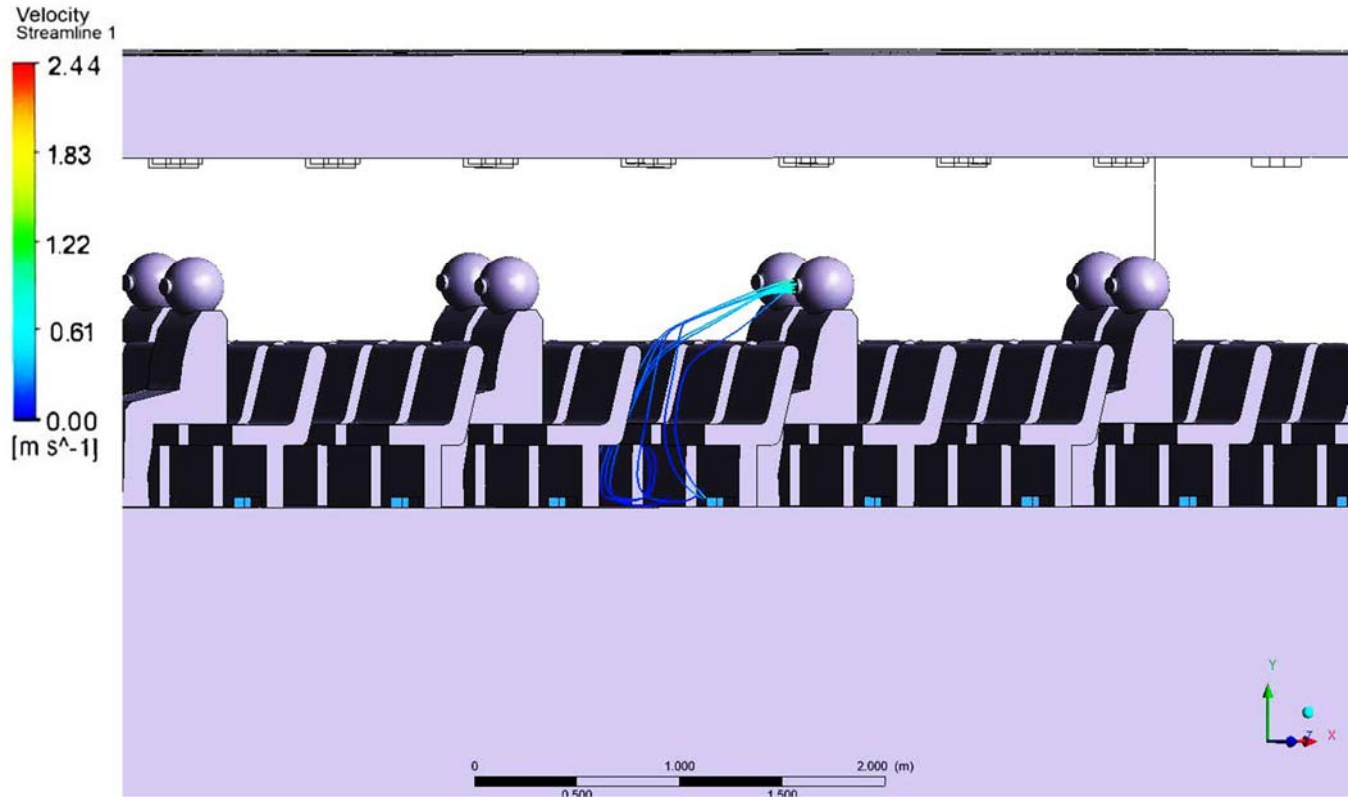
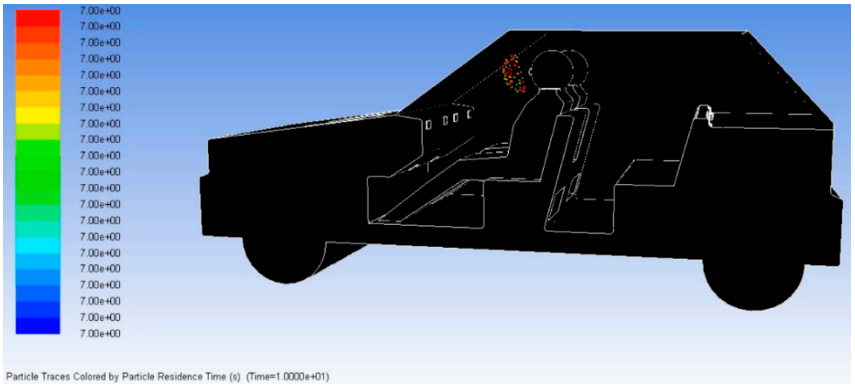
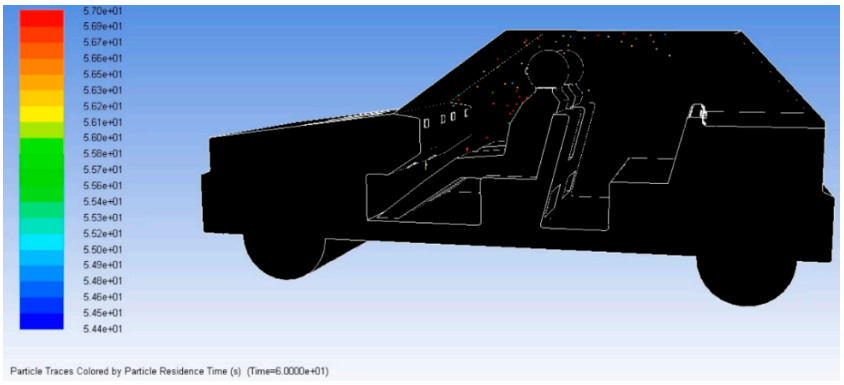


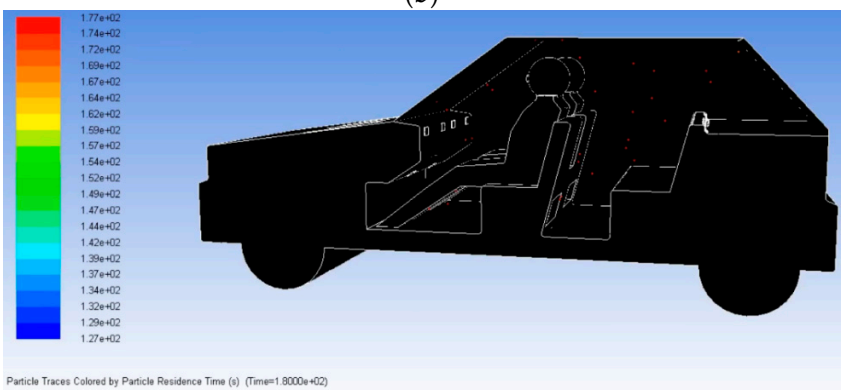
Figure 20. The trajectory of respiration aerosols in the selected typical airplane.



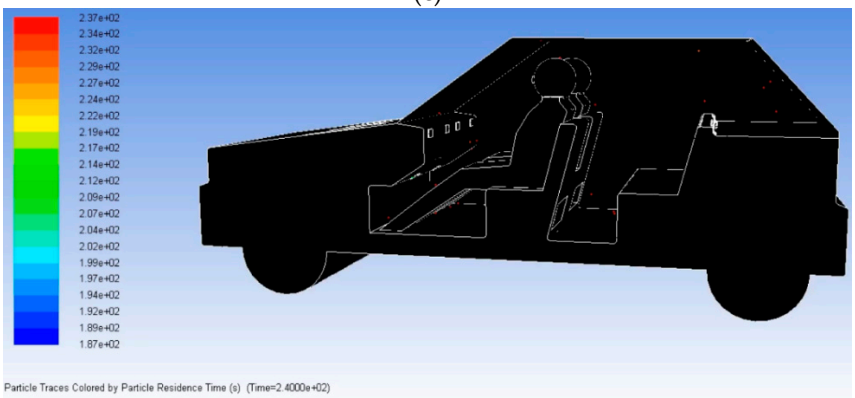
(**a**)



(**b**)

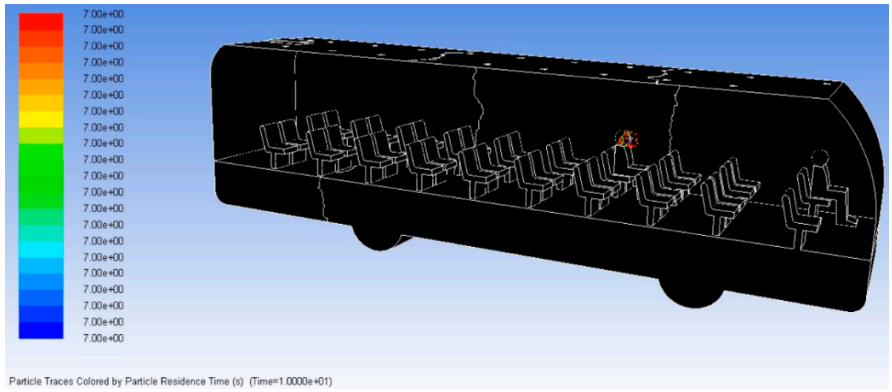


(**c**)

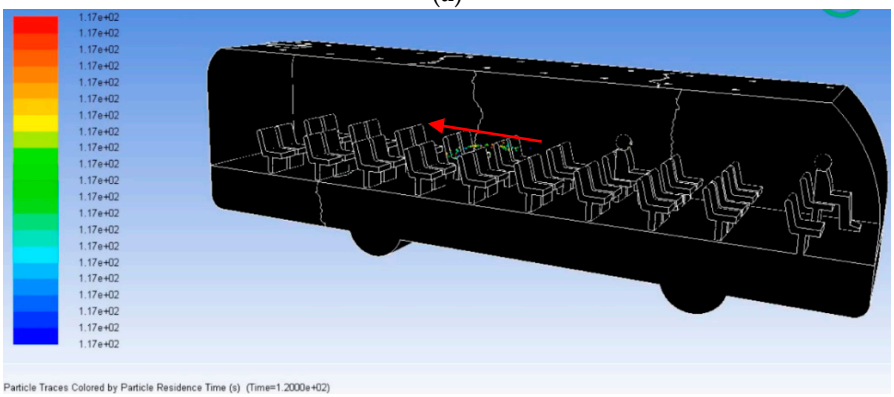


(**d**)

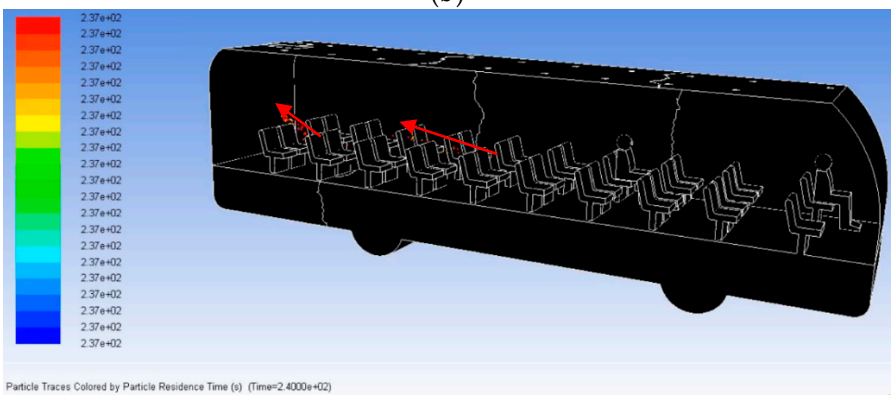
Figure 21. Discrete phase model of the typical car (**a**) 10 s; (**b**) 60 s; (**c**) 180 s; (**d**) 240 s.



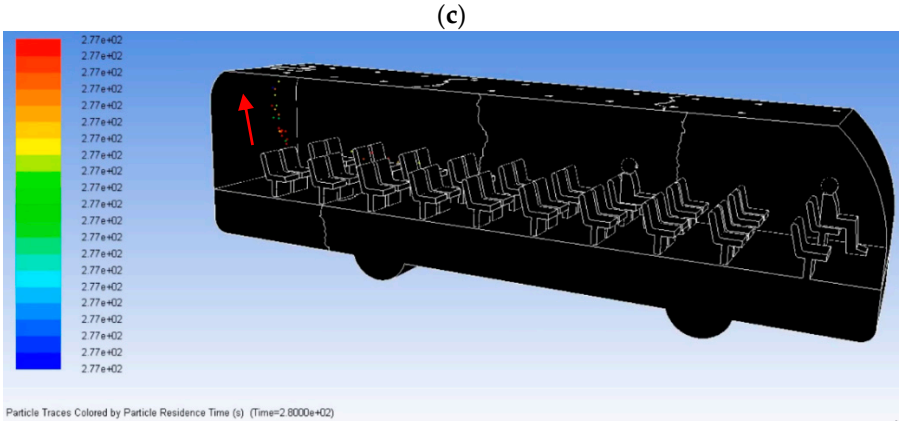
(**a**)



(**b**)

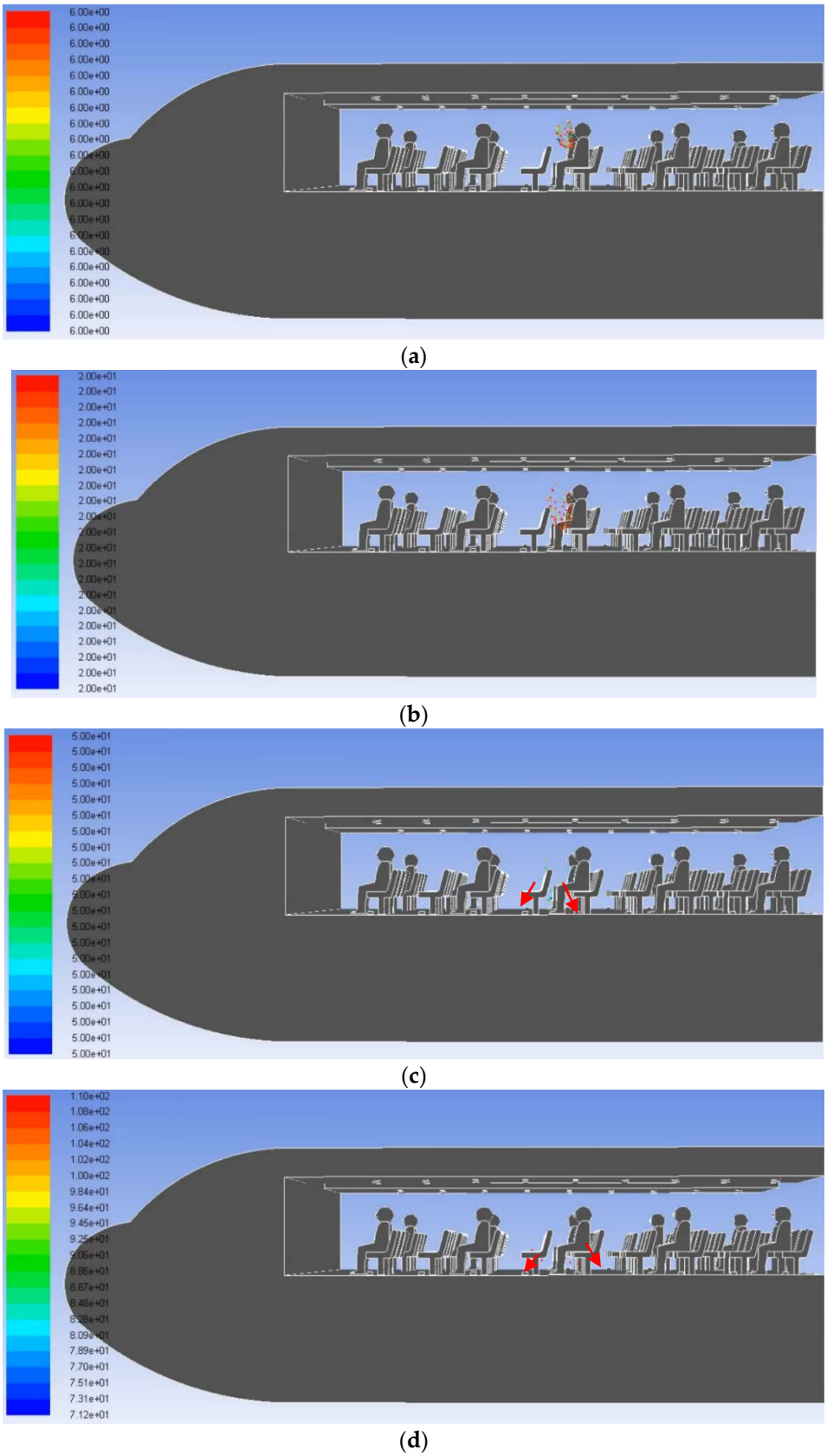


(**c**)



(**d**)

Figure 22. Discrete phase model of the typical bus (**a**) 10 s; (**b**) 120 s; (**c**) 240 s; (**d**) 280 s.



(**a**)

(**b**)

(**c**)

(**d**)

Figure 23. Discrete phase model of the typical airplane (**a**) 10 s; (**b**) 60 s; (**c**) 120 s; (**d**) 240 s.

According to the discrete models, the respiration particles in the car could be circulated in all cabin environments with the HVAC system. In the bus, since the outflow was placed

at the end, the respiration aerosols from the front would pass the entire cabin and reach the end. In the airplane, there were separate outflows under each row, causing restriction of the airflow circulation. Thus, the contaminated respiration particles could have a movement about one–two raw forwards and backwards. In addition, the movement of the contaminated respiration aerosols after just 60 s demonstrated the high risk of an infection event during a few seconds without personal protective equipment (PPE) or during eating/drinking inside the cabins. The estimation of the ACH for the three vehicles is presented in Figure 24.

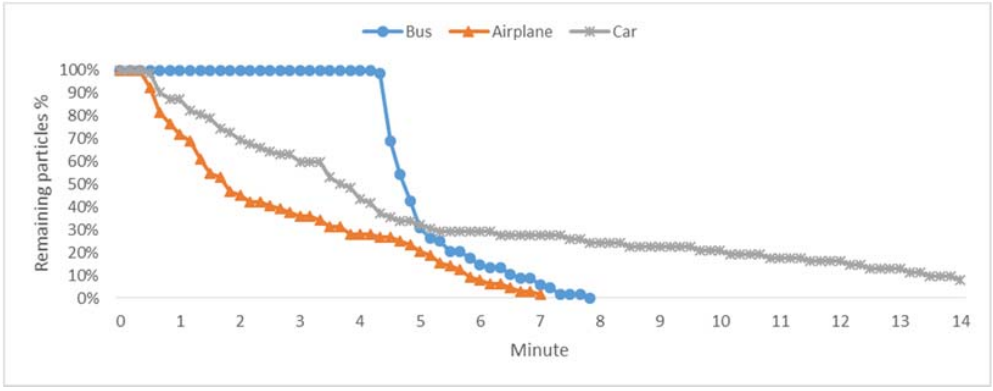


Figure 24. The percentages of the remaining particles in the three selected vehicles.

The graph shows the percentages of the remaining particles over time. The periods for which more than 99% of the particles escaped from the cabins were about 7, 8, and 14 min for the airplane, the bus, and the car, respectively. Therefore, the CFD model analysis determined the ACH for a typical car at about 4.3 (60 min/14 min), a typical bus at about 7.5 (60 min/8 min), and in a typical airplane at about 8.5 (60 min/7.1 min), all less than the minimum protocol of infection prevention at 12 ACH.

4. Conclusions

The analysis exhibited the critical impact of the inflow, the outflow, and the passengers' locations in the cabins. According to the results, the ACH in the three selected vehicles was less than the standard infection prevention protocols, with the lowest in the car at 4.3 and the highest in the airplane at 8.5. The analysis showed that the aerosols in the car could be circulated in all cabin environments with the HVAC system. In the bus, since the outflow was placed at the end, the respiration aerosols from the front would pass the entire cabin to reach the end. The circulation of the aerosols after just 60 s in the entire vehicle's cabin showed a high health risk even during a one-minute stay without PPE.

The analysis showed that the car's opening windows could decrease the contamination loads and improve the low ACH by the HVAC systems. However, for the buses, a new design for the outflow location or an increase in the number of outflows seems necessary. In the case of the airplane, the separate outflows under each row caused a restriction of the airflow circulation. Thus, the possible contaminated respiration aerosols could involve about one row forward and backwards. Since the airflow patterns were suitable in the airplane, it seems that by increasing the airflow rate, the required ACH might be achieved.

In conclusion, the CFD simulations showed that the lowest health risk could be in the airplane and the highest in the bus due to the location of airflows and outflows. Although the simulations in this study were performed for the selected vehicles with specific dimensions, since the boundary conditions are based on several case studies, the main achievements could be valid for similar vehicles.

For future studies, it seems that in the closed AC systems (recirculating), the role of filters in the health risk seems critical and recommended. Furthermore, the current simulation results could improve the indoor air quality in vehicle cabins, besides minimizing

the health risk. Thus, the balance between energy efficiency and health risk in vehicles is suggested for future studies.

Supplementary Materials: The following are available online at https://www.mdpi.com/article/10.3390/su13126799/s1, Video S1: Discrete phase model of aerosols in a typical car, Video S2: Discrete phase model of aerosols in a typical bus, Video S3: Discrete phase model of aerosols in a typical airplane.

Author Contributions: Conceptualization, B.P.; methodology, B.P. and D.M.; software, B.P. and S.N.N.; validation, B.P. and S.N.N.; formal analysis, B.P., S.A.P., and D.M.; investigation, B.P., S.A.P., and M.T.; data curation, B.P., M.T., and S.N.N.; writing—original draft preparation, B.P., S.A.P., and M.T.; writing—review and editing, B.P. and S.A.P. and D.M.; visualization, B.P., S.A.P., and D.M.; supervision, P.P. All authors have read and agreed to the published version of the manuscript.

Funding: This research received no external funding.

Institutional Review Board Statement: Not applicable.

Informed Consent Statement: Not applicable.

Data Availability Statement: Data sharing not applicable.

Conflicts of Interest: The authors declare no conflict of interest.

References

1. Fayazbakhsh, M.A.; Bahrami, M. Comprehensive Modeling of Vehicle Air Conditioning Loads using Heat Balance Method. *SAE Tech. Pap.* **2013**, *2013*, 1507.
2. Marshall, G.J.; Mahony, C.P.; Rhodes, M.J.; Daniewicz, S.R.; Tsolas, N.; Thompson, S.M. Thermal Management of Vehicle Cabins, External Surfaces, and Onboard Electronics: An Overview. *Engineering* **2019**, *5*, 954–969. [CrossRef]
3. Suárez, C.; Iranzo, A.; Salva, J.A.; Tapia, E.; Barea, G.; Guerra, J. Parametric investigation using computational fluid dynamics of the HVAC air distribution in a railway vehicle for representative weather and operating conditions. *Energies* **2017**, *10*, 1074. [CrossRef]
4. Kale, S.R.; Veeravalli, S.V.; Punekar, H.D.; Yelmule, M.M. Air flow through a non-airconditioned bus with open windows. *Sadhana* **2007**, *32*, 347–363. [CrossRef]
5. Mathai, V.; Das, A.; Bailey, J.A.; Breuer, K. Airflows inside passenger cars and implications for airborne disease transmission. *Sci. Adv.* **2021**, *7*, eabe0166. [CrossRef]
6. Gajewski, A. Indoor air quality in a bus. *WIT Trans. Built Environ.* **2013**, *134*, 749–757.
7. Shehadi, M.; Hosni, M.; Jones, B. Airflow and turbulence analysis inside a wide-body aircraft cabin mockup. *Indoor Built Environ.* **2018**, *27*, 766–785. [CrossRef]
8. Haghshenas, S.S.; Pirouz, B.; Haghshenas, S.S.; Pirouz, B.; Piro, P.; Na, K.S.; Cho, S.E.; Geem, Z.W. Prioritizing and analyzing the role of climate and urban parameters in the confirmed cases of COVID-19 based on artificial intelligence applications. *Int. J. Environ. Res. Public Health* **2020**, *10*, 3730. [CrossRef]
9. Pirouz, B.; Haghshenas, S.S.; Haghshenas, S.S.; Piro, P. Investigating a serious challenge in the sustainable development process: Analysis of confirmed cases of COVID-19 (new type of Coronavirus) through a binary classification using artificial intelligence and regression analysis. *Sustainability* **2020**, *12*, 2427. [CrossRef]
10. Pirouz, B.; Haghshenas, S.S.; Pirouz, B.; Haghshenas, S.S.; Piro, P. Development of an assessment method for investigating the impact of climate and urban parameters in confirmed cases of COVID-19: A new challenge in sustainable development. *Int. J. Environ. Res. Public Health* **2020**, *17*, 2801. [CrossRef]
11. Pirouz, B.; Nejad, H.J.; Violini, G.; Pirouz, B. The role of artificial intelligence, MLR and statistical analysis in investigations about the correlation of swab tests and stress on health care systems by COVID-19. *Information* **2020**, *11*, 454. [CrossRef]
12. Lim, T.; Cho, J.; Kim, B.S. The influence of ward ventilation on hospital cross infection by varying the location of supply and exhaust air diffuser using CFD. *J. Asian Archit. Build. Eng.* **2010**, *9*, 259–266. [CrossRef]
13. Abdul Salam, Z.H.; Karlin, R.B.; Ling, M.L.; Yang, K.S. The impact of portable high-efficiency particulate air filters on the incidence of invasive aspergillosis in a large acute tertiary-care hospital. *Am. J. Infect. Control.* **2010**, *40*, S3–S10. [CrossRef]
14. Jankowska, E.; Reponen, T.; Willeke, K.; Grinshpun, S.A.; Choi, K.J. Collection of fungal spores on air filters and spore reentrainment from filters into air. *J. Aerosol Sci.* **2000**, *31*, 969–978. [CrossRef]
15. Holland, M.; Zaloga, D.J.; Friderici, C.S. COVID-19 Personal Protective Equipment (PPE) for the emergency physician. *Vis. J. Emerg. Med.* **2020**, *19*, 100740. [CrossRef] [PubMed]
16. Xu, B.; Chen, X.; Xiong, J. Air quality inside motor vehicles' cabins: A review. *Indoor Built Environ.* **2018**, *27*, 452–465. [CrossRef]
17. Hadei, M.; Mohebbi, S.R.; Hopke, P.K.; Shahsavani, A.; Bazzazpour, S.; Alipour, M.; Jafari, A.J.; Bandpey, A.M.; Zali, A.; Yarahmadi, M.; et al. Presence of SARS-CoV-2 in the air of public places and transportation. *Atmos. Pollut. Res.* **2021**, *12*, 302–306. [CrossRef]

18. Zhu, S.; Demokritou, P.; Spengler, J.D. Field Investigation of Air Quality in University Shuttle Buses. In Proceedings of the 9th International Conference and Exhibition on Healthy Buildings 2009 (HB 09), Syracuse, NY, USA, 13–17 September 2009.
19. Zhu, S.; Srebric, J.; Spengler, J.D.; Demokritou, P. An advanced numerical model for the assessment of airborne transmission of influenza in bus microenvironments. *Build. Environ.* **2012**, *47*, 67–75. [CrossRef]
20. Mazzeo, D.; Matera, N.; de Luca, P.; Baglivo, C.; Congedo, P.M.; Oliveti, G. Worldwide geographical mapping and optimization of stand-alone and grid-connected hybrid renewable system techno-economic performance across Köppen-Geiger climates. *Appl. Energy* **2020**, *276*, 115507. [CrossRef]
21. Mazzeo, D.; Kontoleon, K.J. The role of inclination and orientation of different building roof typologies on indoor and outdoor environment thermal comfort in Italy and Greece. *Sustain. Cities Soc.* **2020**, *60*, 102111. [CrossRef]
22. Baglivo, C.; Mazzeo, D.; Panico, S.; Bonuso, S.; Matera, N.; Congedo, P.M.; Oliveti, G. Complete greenhouse dynamic simulation tool to assess the crop thermal well-being and energy needs. *Appl. Therm. Eng.* **2020**, *179*, 115698. [CrossRef]
23. World Health Organization. *Air Quality Guidelines: For Europe*, 2nd ed.; World Health Organization: Copenhagen, Denmark, 2000.
24. Wargocki, P.; Carrer, P.; de Oliveira Fernandes, E.; Hänninen, O.; Kephalopoulos, S. Guidelines for Health-Based Ventilation in Europe. In Proceedings of the Indoor Air 2014—13th International Conference on Indoor Air Quality and Climate, Hong Kong, China, 7–12 July 2014; pp. 1067–1069.
25. ANSI ANSI/ASHRAE Standard 62.1-2010, Ventilation for Acceptable Indoor Air Quality. Available online: http://arco-hvac.ir/wp-content/uploads/2016/04/ASHRAE-62_1-2010.pdf (accessed on 20 April 2021).
26. Stanke, D.A.; Danks, R.A.; Muller, C.O. Ventilation for acceptable indoor air quality. *Ashrae Stand.* **2010**, *2007*, 1–70.
27. Schwela, D.H.; Haq, G. Strengths and weaknesses of the WHO urban air pollutant database. *Aerosol Air Qual. Res.* **2020**, *20*, 1026–1037. [CrossRef]
28. Nicol, J.F.; Wilson, M. A critique of European Standard EN 15251: Strengths, weaknesses and lessons for future standards. *Build. Res. Inf.* **2011**, *39*, 183–193. [CrossRef]
29. Dimitroulopoulou, C. Ventilation in European dwellings: A review. *Build. Environ.* **2012**, *47*, 109–125. [CrossRef]
30. Zhonghua, Y.; Fang, Y.; Za, Z. Health protection guideline of passenger transport stations and transportation facilities during COVID-19 outbreak. *Chin. J. Prev. Med.* **2020**, *54*, 359–361. [CrossRef]
31. Wu, J.; Weng, W. Transmission of COVID-19 viral particles and the risk of infection among passengers in air-conditioned buses. *J. Tsinghua Univ.* **2021**, *61*, 89–95. [CrossRef]
32. Salari, M.; Milne, R.J.; Delcea, C.; Kattan, L.; Cotfas, L.A. Social distancing in airplane seat assignments. *J. Air Transp. Manag.* **2020**, *89*, 101915. [CrossRef]
33. Talaat, K.; Abuhegazy, M.; Mahfoze, O.A.; Anderoglu, O.; Poroseva, S.V. Simulation of aerosol transmission on a Boeing 737 airplane with intervention measures for COVID-19 mitigation. *Phys. Fluids* **2021**, *33*, 033312. [CrossRef]
34. Eykelbosh, A. Can CO2 Sensors be Used to Assess COVID-19 Transmission Risk? | National Collaborating Centre for Environmental Health | NCCEH—CCSNE. Available online: https://ncceh.ca/content/blog/can-co2-sensors-be-used-assess-covid-19-transmission-risk (accessed on 20 April 2021).
35. Riffi, H. CO2 Sensor Helps to Reduce the Risk of Covid-19 Transmission Indoors—EE Times Europe. Available online: https://www.eetimes.eu/co2-sensor-helps-to-reduce-the-risk-of-covid-19-transmission-indoors/ (accessed on 20 April 2021).
36. Best Indoor Air Quality Monitors 2021 | TechHive. Available online: https://www.techhive.com/article/3356448/best-indoor-air-quality-monitor.html (accessed on 20 April 2021).
37. Hou, J.; Sun, Y.; Dai, X.; Liu, J.; Shen, X.; Tan, H.; Yin, H.; Huang, K.; Gao, Y.; Lai, D.; et al. Associations of indoor carbon dioxide concentrations, air temperature, and humidity with perceived air quality and sick building syndrome symptoms in Chinese homes. *Indoor Air* **2021**. [CrossRef]
38. AHRI COVID Transmission and Air Conditioning Facts. Available online: http://www.ahrinet.org/App_Content/ahri/files/NewsRoom/AHRI-COVID-Report-FAQ.pdf (accessed on 20 April 2021).
39. Xu, H.; Yan, C.; Fu, Q.; Xiao, K.; Yu, Y.; Han, D.; Wang, W.; Cheng, J. Possible environmental effects on the spread of COVID-19 in China. *Sci. Total Environ.* **2020**, *731*, 139211. [CrossRef]
40. Lutz, B.D.; Jin, J.; Rinaldi, M.G.; Wickes, B.L.; Huycke, M.M. Outbreak of invasive Aspergillus infection in surgical patients, associated with a contaminated air-handling system. *Clin. Infect. Dis.* **2003**, *37*, 786–793. [CrossRef] [PubMed]
41. Zhu, S.; Demokritou, P.; Spengler, J. Experimental and numerical investigation of micro-environmental conditions in public transportation buses. *Build. Environ.* **2010**, *45*, 2077–2088. [CrossRef]
42. Liu, W.; Mazumdar, S.; Zhang, Z.; Poussou, S.B.; Liu, J.; Lin, C.H.; Chen, Q. State-of-the-art methods for studying air distributions in commercial airliner cabins. *Build. Environ.* **2012**, *47*, 5–12. [CrossRef]
43. Liu, H.; He, S.; Shen, L.; Hong, J. Simulation-based study of COVID-19 outbreak associated with air-conditioning in a restaurant. *Phys. Fluids* **2021**, *33*, 023301. [CrossRef] [PubMed]
44. Brunetti, G.; Porti, M.; Piro, P. Multi-level numerical and statistical analysis of the hygrothermal behavior of a non-vegetated green roof in a mediterranean climate. *Appl. Energy* **2018**, *221*, 204–219. [CrossRef]
45. Palermo, S.A.; Zischg, J.; Sitzenfrei, R.; Rauch, W.; Piro, P. Parameter Sensitivity of a Microscale Hydrodynamic Model. In *New Trends in Urban Drainage Modelling, UDM 2018*; Mannina, G., Ed.; Green Energy and Technology; Springer: Cham, Switzerland, 2019; pp. 982–987.

46. Piro, P.; Carbone, M. A modelling approach to assessing variations of total suspended solids (TSS) mass fluxes during storm events. *Hydrol. Process.* **2014**, *28*, 2419–2426. [CrossRef]
47. Carbone, M.; Turco, M.; Nigro, G.; Piro, P. Modeling of hydraulic behaviour of green roof in catchment scale. In Proceedings of the International Multidisciplinary Scientific GeoConference Surveying Geology and Mining Ecology Management, Albena, Bulgaria, 17–26 June 2014; Volume 1, pp. 471–477.
48. Turco, M.; Brunetti, G.; Carbone, M.; Piro, P. Modelling the hydraulic behaviour of permeable pavements through a reservoir element model. In Proceedings of the International Multidisciplinary Scientific GeoConference Surveying Geology and Mining Ecology Management, Sofia, Bulgaria, 28 June–7 July 2018; Volume 18, pp. 507–514.
49. Pirouz, B.; Arcuri, N.; Maiolo, M.; Talarico, V.C.; Piro, P. A new multi-objective dynamic model to close the gaps in sustainable development of industrial sector. In *IOP Conference Series: Earth and Environmental Science*; IOP Publishing: Bristol, UK, 2020; p. 012074.
50. Yang, X.; Ou, C.; Yang, H.; Liu, L.; Song, T.; Kang, M.; Lin, H.; Hang, J. Transmission of pathogen-laden expiratory droplets in a coach bus. *J. Hazard. Mater.* **2020**, *397*, 122609. [CrossRef]
51. Yan, Y.; Li, X.; Yang, L.; Yan, P.; Tu, J. Evaluation of cough-jet effects on the transport characteristics of respiratory-induced contaminants in airline passengers' local environments. *Build. Environ.* **2020**, *183*, 107206. [CrossRef]
52. Zhang, B.; Guo, G.; Zhu, C.; Ji, Z. Transport of aerosol by coughing in an air-conditioned space. In Proceedings of the 4th Thermal and Fluids Engineering Conference, Las Vegas, NV, USA, 14–17 April 2019.
53. Yang, L.; Li, X.; Yan, Y.; Tu, J. Effects of cough-jet on airflow and contaminant transport in an airliner cabin section. *J. Comput. Multiph. Flows* **2018**, *10*, 72–82. [CrossRef]
54. Khatoon, S.; Kim, M.H. Thermal comfort in the passenger compartment using a 3-D numerical analysis and comparison with Fanger's comfort models. *Energies* **2020**, *13*, 690. [CrossRef]
55. Fišer, J.; Pokorný, J. Effect of car speed on amount of air supplied by ventilation system to the space of car cabin. In *EPJ Web Conferences*; EDP Sciences: Ulis, France, 2014; pp. 201–204.
56. Alexandrov, A.; Kudriavtsev, V.; Reggio, M. Analysis of Flow Patterns and Heat Transfer in Generic Passenger Car Mini-Environment Managing Director. In Proceedings of the 9th Annual Conference of the CFD Society of Canada, Kitchener, ON, Canada, 27–29 May 2001.
57. Danca, P.; Bode, F.; Nastase, I.; Meslem, A. CFD simulation of a cabin thermal environment with and without human body—Thermal comfort evaluation. In *E3S Web of Conferences*; EDP Sciences: Ulis, France, 2018; p. 01018.
58. Bilgili, M.; Aktas, A.E.; Cardak, E. Thermodynamic Analysis of Bus Air Conditioner Working with Refrigerant R600a. *Eur. Mech. Sci.* **2017**, *1*, 69–75. [CrossRef]
59. Yang, H.; Wang, Y.; He, T. The Analysis on the Effect of Passenger Car Air Conditioning and Distribution with Different Inlet Parameters. In Proceedings of the First International Conference on Information Sciences, Machinery, Materials and Energy, Chongqing, China, 11–13 April 2015.
60. Gürbüz, H.; Akçay, I.H.; Asghar, H.; Ali, Q.A. Analysis of bus air conditioning system by finite elements method (ANSYS). *Int. J. Automot. Eng. Technol.* **2016**, *5*, 115–124. [CrossRef]
61. Garner, R.P.; Wong, K.L.; Ericson, S.C.; Baker, A.J.; Orzechowski, J.A. CFD validation for contaminant transport in aircraft cabin ventilation flow fields. In Proceedings of the Proceedings—Annual SAFE Symposium, Maastricht, The Netherlands, 15–18 June 2003.
62. Müller, C.; Scholz, D.; Giese, T. Dynamic simulation of innovative aircraft air conditioning. In Proceedings of the First CEAS European Air and Space Conference, Berlin, Germany, 10–13 September 2006.
63. You, R.; Chen, J.; Shi, Z.; Liu, W.; Lin, C.H.; Wei, D.; Chen, Q. Experimental and numerical study of airflow distribution in an aircraft cabin mock-up with a gasper on. *J. Build. Perform. Simul.* **2016**, *9*, 555–566. [CrossRef]
64. Rai, A.C.; Chen, Q. Simulations of ozone distributions in an aircraft cabin using computational fluid dynamics. *Atmos. Environ.* **2012**, *54*, 348–357. [CrossRef]
65. Wang, J.X.; Cao, X.; Chen, Y.P. An air distribution optimization of hospital wards for minimizing cross-infection. *J. Clean. Prod.* **2021**, *279*, 123431. [CrossRef]
66. Yan, Y.; Li, X.; Shang, Y.; Tu, J. Evaluation of airborne disease infection risks in an airliner cabin using the Lagrangian-based Wells-Riley approach. *Build. Environ.* **2017**, *121*, 79–92. [CrossRef]
67. Abuhegazy, M.; Talaat, K.; Anderoglu, O.; Poroseva, S.V.; Talaat, K. Numerical investigation of aerosol transport in a classroom with relevance to COVID-19. *Phys. Fluids* **2020**, *32*, 103311. [CrossRef]
68. Ahn, J.; Choi, H.Y. Effects of Supply Angle on Thermal Environment of Residential Space with Hybrid Desiccant Cooling System for Multi-Room Control. *Appl. Sci.* **2020**, *10*, 7271. [CrossRef]
69. Zhang, C.; Bounds, C.P.; Foster, L.; Uddin, M. Turbulence modeling effects on the CFD predictions of flow over a detailed full-scale sedan vehicle. *Fluids* **2019**, *4*, 148. [CrossRef]
70. Dong, H.; Qin, Z.; Liu, S.; Li, Y.; Shen, Y.; Wang, H.; Zong, Y.; Wu, X.; Si, H. Numerical investigation into the air flow distributions of the air conditioning system in the modular data center. *Adv. Appl. Math. Mech.* **2019**, *11*, 91–107. [CrossRef]
71. Ng, K.C.; Kadirgama, K.; Ng, E.Y.K. Response surface models for CFD predictions of air diffusion performance index in a displacement ventilated office. *Energy Build.* **2008**, *40*, 774–781. [CrossRef]
72. Zhu, S.; Dalgo, D.; Srebric, J.; Kato, S. Cooling efficiency of a spot-type personalized air-conditioner. *Build. Environ.* **2017**, *121*, 35–48. [CrossRef]